



## RESEARCH ARTICLE

10.1029/2019MS001633

## Decadal Stabilization of Soil Inorganic Nitrogen as a Benchmark for Global Land Models

## Key Points:

- Soil inorganic nitrogen showed large spatial heterogeneity across China
- No temporal trend of soil inorganic nitrogen concentration was detected across China during the past three decades
- Large biases exist when estimating the soil inorganic nitrogen pool in current global land models

## Supporting Information:

- Supporting Information S1

## Correspondence to:

J. Xia,  
jyxia@des.ecnu.edu.cn

## Citation:

Wei, N., Cui, E., Huang, K., Du, Z., Zhou, J., Xu, X., et al. (2019). Decadal stabilization of soil inorganic nitrogen as a benchmark for global land models. *Journal of Advances in Modeling Earth Systems*, 11, 1088–1099. <https://doi.org/10.1029/2019MS001633>

Received 27 JUL 2018

Accepted 28 MAR 2019

Accepted article online 05 APR 2019

Published online 17 APR 2019

Ning Wei<sup>1</sup>, Erqian Cui<sup>1</sup>, Kun Huang<sup>1</sup>, Zhenggang Du<sup>1</sup>, Jian Zhou<sup>1</sup>, Xiaoni Xu<sup>1</sup>, Jing Wang<sup>1</sup>, Liming Yan<sup>1</sup>, and Jianyang Xia<sup>1,2</sup>

<sup>1</sup>Zhejiang Tiantong Forest Ecosystem National Observation and Research Station, Shanghai Key Lab for Urban Ecological Processes and Eco-Restoration, School of Ecological and Environmental Sciences, East China Normal University, Shanghai, China, <sup>2</sup>State Key Laboratory of Estuarine and Coastal Research, Research Center for Global Change and Ecological Forecasting, East China Normal University, Shanghai, China

**Abstract** Global land models are now routinely incorporating the nitrogen (N) cycle into simulations, but the identification of its benchmarks has lagged behind. An important variable in these models is the soil inorganic N (SIN) which is the resultant of different input and output N processes. However, whether and how the SIN pool and its spatiotemporal variation can be used as benchmarks for models remains unclear. Here we first constructed a database of measured SIN at 756 sites from 1980 to 2010 across China, one of the regions that has been experiencing the highest external N input. Although there was great spatial variability of the measured SIN pool, no significant changes were detected across China during 1980–2010 based on a bootstrapping approach. The medians of the measured SIN across China were 63, 70, and 65 mg/kg during the 1980s, 1990s, and 2000s, respectively. Then, we used the regional SIN database to evaluate two versions of the Community Land Model (i.e., CLM4.5 and CLM5.0). In comparison with the observation (median 75 mg/kg) at grid-cell scale, both CLM4.5 (median 0.70 mg/kg) and CLM5.0 (median 0.79 mg/kg) underestimated the SIN pools across China. Although the drivers of such modeling biases are difficult to identify at the current stage, improved representations of both input and output processes of the SIN pool in the models are highly recommended. These findings suggest that a decadal stabilization of the SIN pool in terrestrial ecosystems and the spatial distribution of the SIN pool may be a useful benchmark for global biogeochemical models.

## 1. Introduction

Nitrogen (N) availability is tightly coupled to terrestrial carbon (C) cycle through stoichiometry and is therefore critical in regulating the feedback between the biosphere and climate change in the Earth system (Hungate et al., 2003; Luo et al., 2004; Peñuelas et al., 2013; Wang & Houlton, 2009). However, our current projections on future climate change are mainly from some Earth system models (ESMs), which neglect the terrestrial N cycle (Wieder et al., 2015). Thus, incorporating terrestrial N processes into ESMs is now highly encouraged (Hurrell et al., 2013; Luo et al., 2016). The addition of C-N interactions into global land models usually lead to reduced terrestrial C uptake and storage (Thornton et al., 2009; Wang & Pak, 2010; Wieder et al., 2015; Zaehle et al., 2014). However, the existing modeling schemes for the C-N interaction are so different (Du et al., 2018) that they could further enlarge the uncertainty of the C cycle projection in current ESMs (Friedlingstein et al., 2006, 2014). Hence, developing useful benchmarks for model performances on the N cycling is urgently needed.

Benchmarking the performance of coupled C-N cycle models is difficult because the N cycle is openly driven by multiple processes that simultaneously compete for soil inorganic N (SIN; Niu et al., 2016; Zhu et al., 2017). For example, when the SIN pool increases, soil N losses such as those due to gaseous emissions and leaching increase exponentially, but biological N fixation is weakened hyperbolically (Aber et al., 1998). N uptake by plants (Hajari et al., 2014) and mineralization by microbes (Delgadobaquerizo & Gallardo, 2011) are both stimulated by SIN increases, but then they approach a maximum or even level off once the SIN pool is saturated (Hajari et al., 2014). However, because the pool size of SIN is much smaller than that of the organic N pools (Schlesinger & Bernhardt, 2013), its observations are usually reported without further analyses in the previous studies. Thus, it remains unclear whether the observations of SIN could be a helpful benchmark for global C-N-coupled models.

©2019. The Authors.

This is an open access article under the terms of the Creative Commons Attribution-NonCommercial-NoDerivs License, which permits use and distribution in any medium, provided the original work is properly cited, the use is non-commercial and no modifications or adaptations are made.

The SIN pool may be a useful benchmark for model performance due to at least two reasons. First, abundant individual measurements on SIN have been conducted in recent decades with comparable quantitative methods (Keeney, 1982). Hence, the observations of SIN are more available, and its methodological uncertainty is smaller than that of other N-related variables or processes. Second, the competition for SIN among multiple N processes is a fundamental mechanism in most existing C-N-coupled models (Du et al., 2018; Hurrell et al., 2013; Thornton et al., 2009; Wang & Pak, 2010; Zaehle & Friend, 2010). Thus, the size of SIN may be the first critical step to understand the emergent pattern of N limitation effect on global C cycle.

It is still unknown whether the SIN pool and its spatiotemporal variations can be useful benchmarking for the C-N-coupled models. Once the SIN pool is replenished by lighting, biological fixation (Dommergues & Ganry, 1986), or bedrock weathering (Houlton et al., 2018), it is quickly absorbed by plants (Xia & Wan, 2008), or it leaves the soil via denitrification (Jorgensen, 1993), volatilization, or leaching (Dise & Wright, 1995). As a result, the SIN pool is highly fluctuating on the short time scale (Cain et al., 1999). However, it is unclear how the regional-scale SIN pool changes on a long-term time scale (Gruber & Galloway, 2008), especially under enhanced global environmental changes in recent decades (Galloway et al., 2008; Greaver et al., 2016). The database of SIN covered a large area, and a long time scale is still inaccessible to quantitatively evaluate the spatiotemporal variations of SIN.

In this study, we first established a comprehensive data set of SIN in China over three decades (from 1980s to 2000s) by collecting all the available SIN data from the National Research Network of China (CNERN) and the published literature. Then, we used the regional data set to evaluate the performance of two state-of-the-art global land surface models (i.e., CLM4.5 and CLM5.0). The specific aims of this study are to (1) explore whether and how the SIN pool changes over time on a regional scale and (2) evaluate the performance of current global land surface models in simulating soil N availability.

## 2. Materials and Methods

### 2.1. Database of In Situ Measurements

We collected SIN data (1990–2008) from the CNERN. In addition, ancillary information, such as latitude, longitude, soil sampling depth, and sampling seasons, were also extracted. The main information of these sites is shown in supporting information Table S1. Furthermore, peer-reviewed literature related to SIN published during 1980–2010 was searched using the China National Knowledge Infrastructure ([www.cnki.net](http://www.cnki.net)). The selected studies must directly report the SIN or provided both ammonium and nitrate N contents. Original SIN data were collected from reported tables, extracted from graphs by the GetData Graph Digitizer software, or calculated as the sum of  $\text{NH}_4^+$ -N plus  $\text{NO}_3^-$ -N. All the collected SIN data should represent the basic soil fertility at the sampling sites. Therefore, we only adopted the measurements in natural conditions (the controlled group) to avoid the impacts from other manipulations. The SIN data sampled from different soil depths was averaged and considered as the basic SIN status at each sampling site. Based on the site descriptions or the dominant vegetation type, studies were classified into forest, grassland, shrubland, desert, cropland, wetland, and bare ground. The influence from land use history was not considered in our study. We obtained geographical coordinates from Google Earth based on the name or description in the case that it was not reported. Overall, the compiled database contained 1,853 records from the CNERN and 3,204 records from 728 published studies (Figure 1).

### 2.2. Statistical Analysis

A complete spatial randomness (CSR) analysis was applied to test the spatial distributions of data points in different decades (Figure S1). Under the null hypothesis of CSR (Baddeley, 2007; Morales et al., 2014), the theoretical value ( $G_{\text{CSR}}$ ) was calculated as

$$G_{\text{CSR}}(r) = 1 - \exp(-\lambda\pi r^2), \quad (1)$$

where  $r$  is the distance of each data point to its nearest neighbor, and  $\lambda$  is the number of data points per unit area. We estimated the observational  $G_{\text{ob}}(r)$  based on the cumulative frequency distribution of  $r$ . To analyze whether  $G_{\text{ob}}(r)$  deviated from  $G_{\text{CSR}}(r)$ , we used a Monte Carlo simulation to calculate the confidence bands around  $G_{\text{CSR}}(r)$ . If  $G_{\text{ob}}(r)$  was within the confidence bands, the spatial points pattern obeyed CSR. If  $G_{\text{ob}}(r)$  was above (below) the confidence bands, the spatial distribution of points was an aggregation (a regulation).

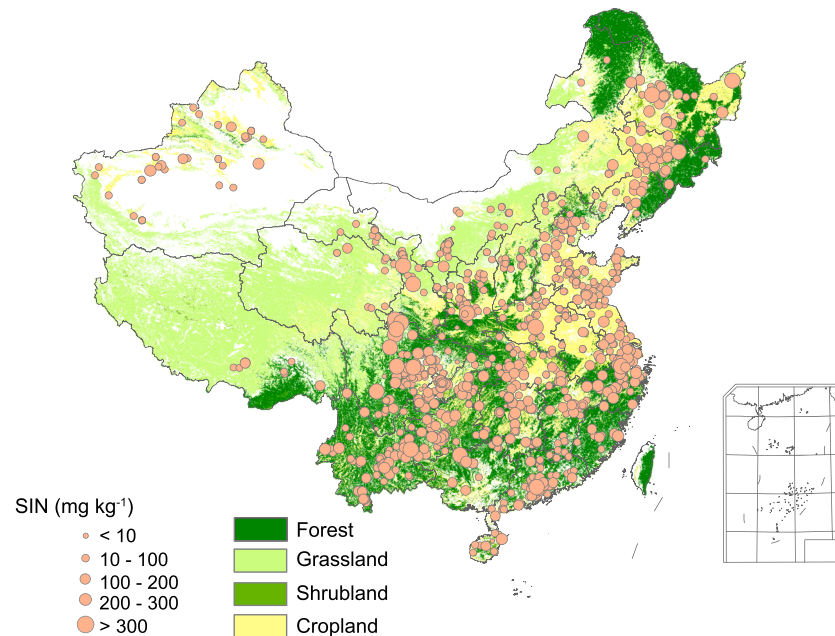


**Figure 1.** The spatial distribution of all the data points in different biomes. The size of the circle indicates the annual mean content of SIN at the site. SIN = soil inorganic nitrogen.

The observational  $G_{ob}(r)$  was above the confidence band in the 1980s, 1990s, and 2000s, which indicated the similar spatial distributions of data points in these three decades (Figure S2). Thus, we assumed that the sampling bias resulting from the spatial distribution of data points was within the acceptable limit.

We then used a simple 5-year moving average to smooth out short-term variation and analyzed the long-term trends of SIN during the period of 1980–2010. The contents of each 5-year database change were in the following ordered datum stream:

$$SIN_{sub(n-1979)} = SIN_{yr(n)} + SIN_{yr(n+1)} + SIN_{yr(n+2)} + SIN_{yr(n+3)} + SIN_{yr(n+4)}, \quad (2)$$

where  $n \in [1980, 2006]$ . For each 5-year database, 1,000 times bootstrapping was applied to generate the sub-database. We then calculated the median values and the 25th and 75th percentiles for each sub-database. To test the decadal trends of the SIN pool across China, all the data of the observations were separated into three decades. Instead of mean values, we applied medians because of its typical representation of data set with extremely large and small values. The range of 25th percentile to 75th percentile was used to indicate the variations.

Given different site climate conditions may have potential effects on SIN, we further downloaded global climate data (temperature and precipitation) across 1980 to 2005 from online sources ([https://crudata.uea.ac.uk/cru/data/hrg/cru\\_ts\\_3.23/](https://crudata.uea.ac.uk/cru/data/hrg/cru_ts_3.23/)). The annual mean values of temperature and precipitation were then calculated. To match the climate data with the sampling sites, the extraction tool in ESRI ArcGIS 10.1 (extraction to points) was applied based on the corresponding latitude and longitude. The effects of temperature and precipitation on spatial SIN variation were detected by general linear models.

To evaluate the responses of SIN pool under climate change, we renewed the data set of Lu et al. (2011), Bai et al. (2013), and Liang et al. (2016) and applied the meta-analysis to calculate the general responses of the SIN pool to CO<sub>2</sub> rising, N addition, and warming:

$$R = \ln \frac{X_E}{X_C} = \ln(X_E) - \ln(X_C), \quad (3)$$

where  $X_E$  is the measured SIN under the treatments (CO<sub>2</sub> enrichment, N addition, and warming), and  $X_C$  is

that from the controlled plots. The response ratio ( $R$ ) is an index of the effect size of treatments (Hedges et al., 1999). The variance ( $Var$ ) of  $R$  is calculated as

$$Var = \frac{S_E^2}{n_E X_E^2} + \frac{S_C^2}{n_C X_C^2}, \quad (4)$$

where  $S_E$  and  $S_C$  are the standard deviation of  $X_E$  and  $X_C$ .  $n_E$  and  $n_C$  are the sample size of treatments and control plots. The weighted response ratio ( $R_{++}$ ) and its variance ( $Var_{++}$ ) were calculated as

$$w = \frac{1}{Var}, \quad (5)$$

$$R_{++} = \frac{\sum_{j=1}^k w_j R_j}{\sum_{j=1}^k w_j}, \quad (6)$$

$$Var_{++} = \frac{1}{\sum_{j=1}^k w_j}, \quad (7)$$

where  $w$  represents the weighting factor of each study;  $k$  is the number of studies. The 95% confidence interval (95% CI) of  $RR_{++}$  was estimated by

$$95\%CI = R_{++} \pm 1.96Var_{++}. \quad (8)$$

The effects of treatment on SIN pool were considered as significant when 95% CI did not overlap with zero (Xia & Wan, 2008).

### 2.3. Simulation of SIN by the CLM and Data-Model Comparison

The Community Land Model (CLM) is the land part of the Community Earth System Model (CESM), which has explicitly implemented the terrestrial N cycle (Oleson et al., 2013). Vertical nutrient mixing processes in the soil profile were included in the versions 4.5 and 5.0 of CLM (CLM4.5 and CLM5.0; Koven et al., 2013). We ran the two versions of CLMs at  $1^\circ \times 1^\circ$  resolution. Same historical climate forcing data set Global Soil Wetness Project Phase 3 (GSWP3) from 1980 to 2005 (<http://hydro.iis.u-tokyo.ac.jp/GSWP3/>) was used to drive the models. Relevant variables were outputted for further model-data comparison.

CLM volume-based SIN ( $\text{g/m}^3$ ) in different depths of soil layers was transformed to weight-based SIN ( $\text{mg/kg}$ ) by the following equation:

$$SIN(\text{mg/kg}) = \frac{SIN(\text{g/m}^3) \times 1,000}{BD(\text{kg/m}^3)}, \quad (9)$$

where  $BD$  is the corresponding soil bulk density in the soil depth from CLM. According to the frequency distribution of the sampling soil depths in the observational data set (Figure S6), the SIN data sampled from top 0–40 cm soil accounted for 87.2%. Besides, the changes of SIN along soil depths showed that abundant SIN was accumulated in the top 0–40 cm soil (Figure S6). We then averaged the top 0–40 cm weight-based SIN ( $\text{mg/kg}$ ) from CLM. Given models operated at grid-cell scale, the simulated SIN represented the average status across the whole grid cell. However, the observed SIN data were from point-scale measurements. To reconcile the scale mismatch, we averaged the observed data within each CLM grid cell before the model-data comparison at different time and space scales.

The simulated SIN data from 1980 to 2005 was averaged and then compared with the observed SIN at grid-cell scale. To estimate whether models can capture different SIN statuses among ecosystems or not, we further considered the observed SIN variations among ecosystems as benchmarks for models. The classification of ecosystem type was based on the information from the observational data set. Given SIN shows great variations throughout seasons, we also benchmarked the seasonal variations of simulated SIN. According to the definition of meteorological seasons in northern hemisphere, we classified the observed SIN data into different sampling seasons: spring (from March to May), summer (June to August), autumn (September to

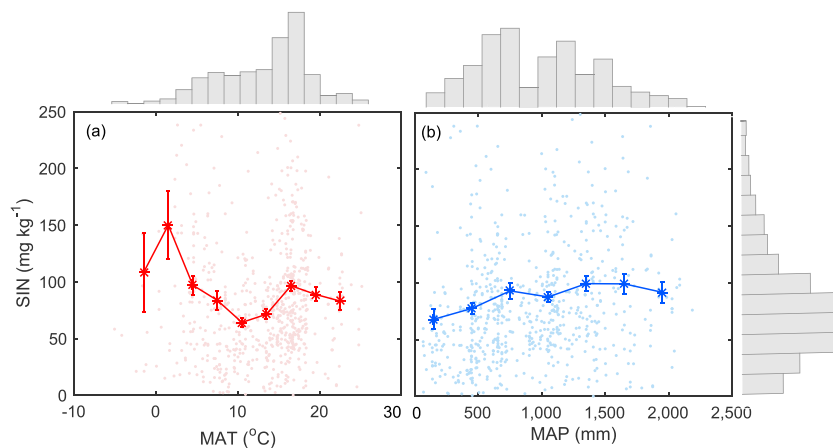


**Figure 2.** The changes in SIN concentrations with the increase in temperature (a) and precipitation (b). SIN shows a significant correlation with precipitation ( $y = 0.018x + 71.29$ ,  $p < 0.001$ ). The histograms along the axes show the relative distribution of corresponding data. MAT = mean annual temperature; MAP = mean annual precipitation; SIN = soil inorganic nitrogen.

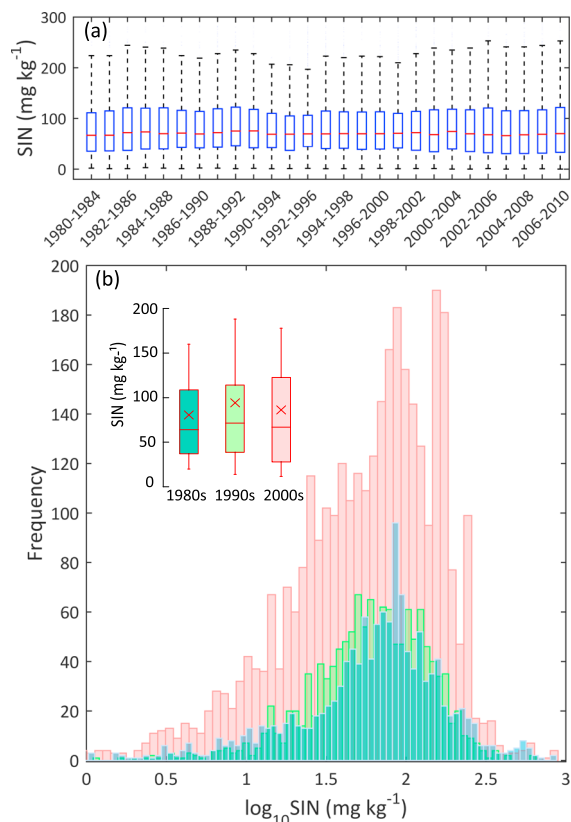


**Figure 3.** The temporal trends of the SIN in China's soil. (a) The annual trend of SIN in China's soil over a 5-year moving window. For each 5-year database, 1,000 times bootstrapping was applied to generate the subdatabase. The red lines represent the medians. The lower and upper edges of the boxes indicate the 25th and 75th percentiles, respectively. Bars outside the boxes represent the 10th and 90th percentiles of the subdatabase. (b) The frequency of the SIN data after transformed into  $\log_{10}$  values in three decades. The inserted boxplots represent SIN status in three decades. SIN = soil inorganic nitrogen.

November), and winter (from December to February). The simulated SIN data were classified and averaged for each season throughout the simulation years accordingly before the model-data comparison.

To estimate the simulated SIN trends from 1980 to 2005 explicitly over a large spatial scale, we used least squares methods to diagnose the changes in the SIN in each grid cell:

$$\text{SIN}(\text{year}) = k \times \text{year} + b, \quad (10)$$

where the SIN (year) is the annual mean SIN in the corresponding year (from 1980 to 2005).  $k$  and  $b$  are the fitting parameters. The value of each grid in the trends map is the corresponding gradient  $k$ .

Influxes and effluxes of the SIN pool were averaged over 26 years for further detection. To understand the changes in SIN with the variation of net fluxes, the simulated SIN was then correlated with influxes minus effluxes. Before the application of regression, data were 5,000-time bootstrapped under a 3-year moving window and averaged to stabilize variation.

### 3. Results

#### 3.1. Spatial and Temporal Patterns of SIN Across China

The measured SIN over 1980 to 2010 showed a strong spatial variation across China, with a broad range from 0.12 to 894 mg/kg (Figure 1). We then used the difference between the upper (75th) and lower (25th) quartiles as an indicator of the spatial variability of SIN across China in each year. Based on the moving-window analysis with a bootstrapping approach, a linear and significant increase ( $+11.7\%$ ;  $R^2 = 0.33$ ,  $p < 0.05$ , Figure S3b) in the spatial variation of SIN was detected from 1980–1984 to 2006–2010. The mean SIN concentration reached its highest value (149.9 mg/kg) in regions with MAT around 1 °C and was lowest at approximately 10 °C MAT (64.2 mg/kg; Figure 2a). The spatial SIN variation had a significant correlation with MAP ( $p < 0.001$ , Figure 2b).

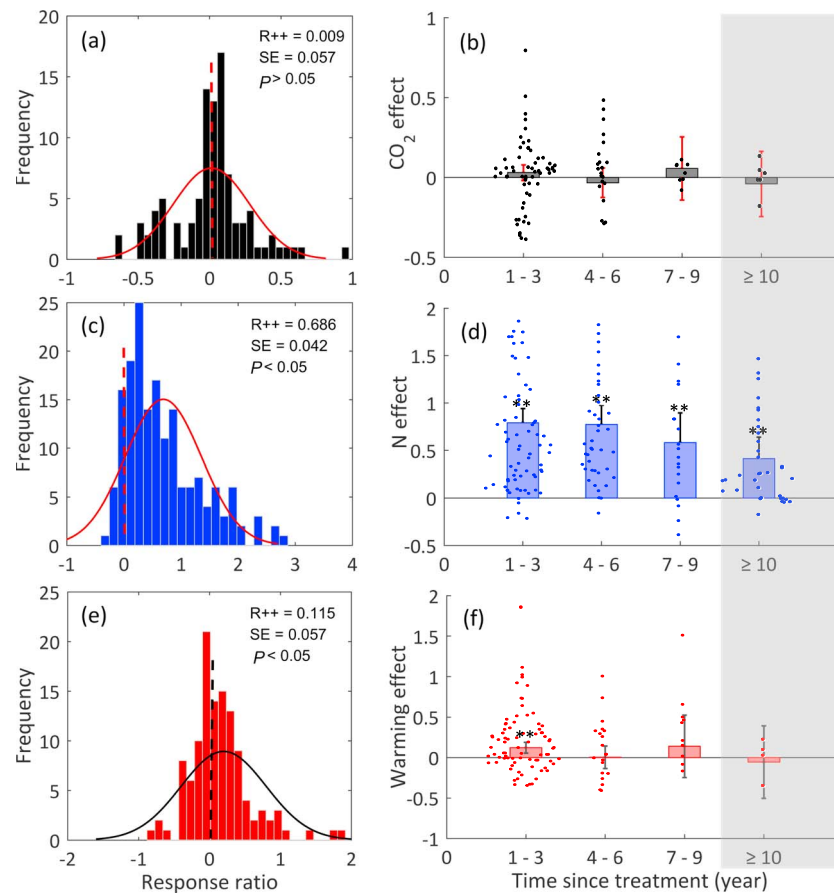


**Figure 4.** The frequency distribution of overall CO<sub>2</sub> (a), nitrogen loading (c), and warming (e) effects on SIN pool. The solid curves show the Gaussian distribution fits. The dashed line marks effects equal 0 ( $R = 0$ ). The weighted response ratio ( $R_{++}$ ) of SIN to CO<sub>2</sub> (b), nitrogen (d), and warming (f) changes with the increase of experimental duration. The circles are the response ratio ( $R$ ) of individual studies. Statistically significant effects on SIN pool are marked with two asterisks. The shaded area shows the response at decadal scale. SIN = soil inorganic nitrogen.

However, no trend of the SIN concentration across China was detected on the temporal scale from 1980 to 2010 (Figure 3a). In 89% of the 5-year moving windows, the median values of the annual SIN changed within  $70 \pm 3$  mg/kg (Figure S3a). On the decadal scale, the median values of SIN across China were 63.02 mg/kg ( $n = 1,185$ ), 70.41 mg/kg ( $n = 825$ ), and 65.43 mg/kg ( $n = 3,123$ ) over the 1980s, 1990s, and 2000s, respectively (Figure 3b).

### 3.2. Experimental Responses of SIN to Environmental Changes

The results from meta-analysis showed an insignificant effect of elevated CO<sub>2</sub> on the SIN pool from annual to decadal time scales (Figures 4a and 4b). N addition significantly increased the SIN pool by 101.2% when integrated all experiments (Figure 4c), but the positive effect decreased with the experimental duration increasing (Figure 4d). Some of the long-term (e.g., >10 years) N loading experiments displayed a neutral effect on the SIN pool (Figure 4d). Experimental warming significantly stimulated the SIN pool by 15.5% across the 118 records (Figure 4e). However, such a positive effect was only found in short-term (i.e., 1–3 years) experiments (Figure 4f).

### 3.3. Benchmarking Model Simulations Against SIN Observations

At grid-cell scale, CLM4.5 and CLM5.0 both significantly underestimated the SIN pool across China from 1980 to 2005 (Figure 5, Kruskal-Wallis test, both  $p < 0.01$ ). The SIN concentrations across China were simulated as 0.70 (0.40, 1.19) mg/kg (median (25th percentile, 75th percentile)) and 0.79 (0.29, 2.40) mg/kg by

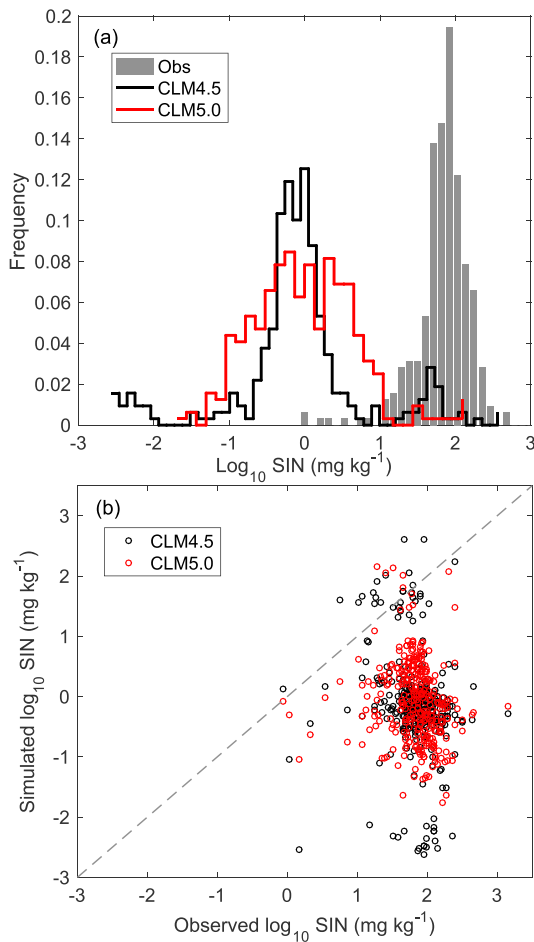


**Figure 5.** (a) The frequency of the SIN conditions in observations and the models' simulations. (b) The simulated SIN from CLM4.5 and CLM5.0 against observational SIN. The dark open circles represent CLM4.5 simulations, and the red represent CLM5.0. The dashed line is the 1:1 line. SIN = soil inorganic nitrogen; CLM = Community Land Model.

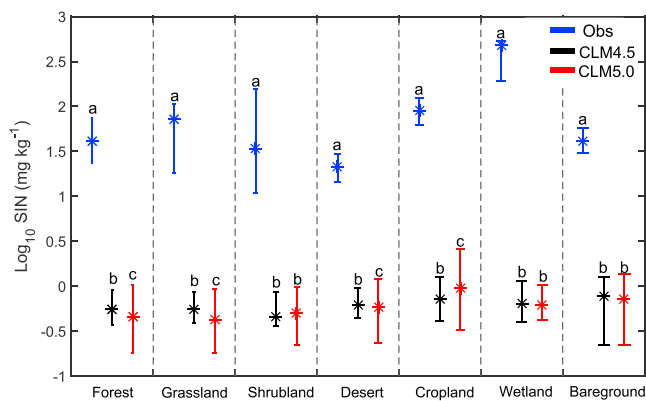


**Figure 6.** The simulated SIN conditions in different ecosystems from CLM4.5 and CLM5.0 against observations. Under the same ecosystem type, the unique letters above error bars indicate significant differences ( $P < 0.05$ ) between groups. The asterisks show the medians among ecosystems, and the lower and upper error bars indicate the 25th and 75th percentiles. SIN = soil inorganic nitrogen; CLM = Community Land Model.

CLM4.5 and CLM5.0, respectively, both of which were dramatically lower than the observations 75.00 (49.16, 105.30) mg/kg (Figure 5a). Both  $\text{NH}_4^+\text{-N}$  and  $\text{NO}_3^-\text{-N}$  concentrations were underestimated by two models (Figure S5). The simulated overall SIN concentrations from CLM4.5 and CLM5.0 showed no significant difference ( $p = 0.28$ , Figure 5). However, CLM4.5 simulated a larger  $\text{NH}_4^+\text{-N}$  concentration, while CLM5.0 simulated a larger  $\text{NO}_3^-\text{-N}$  concentration.

The underestimation of SIN concentration by the two models existed in all types of ecosystems in China (Figure 6). The observed SIN concentration varied greatly among different ecosystems, with the medians ranged from 21.47 (14.45, 29.93) mg/kg (median (25th percentile, 75th percentile)) in desert to 475.19 (215.12, 539.93) mg/kg in wetland. The SIN concentration in cropland reached 90.54 (62.54, 125.59) mg/kg. SIN status in grassland (71.95 (18.34, 105.82) mg/kg) was secondary to cropland. The median SIN concentration was 40.92 (23.73, 74.97) mg/kg in forest and 34.01 (10.82, 154.83) mg/kg in shrubland. With limited observations, the SIN concentration in bare ground was 41.37 (30.05, 58.05) mg/kg. Models failed to simulate the variations of SIN among different ecosystems. We then further compared the simulated results between the two models. As shown by the Kolmogorov-Smirnov test, SIN statuses simulated from CLM4.5 and CLM5.0 showed no significant difference in shrubland, wetland, and bare ground (Figure 6). The CLM4.5 model simulated a larger median SIN concentration in forest and grassland than the CLM5.0 model ( $p < 0.05$ ).

The observed SIN concentration in summer was the lowest throughout seasons with a relatively small variation, 61.42 (31.52, 94.10) mg/kg (median (25th percentile, 75th percentile)). The SIN concentration in spring was 73.08 (40.71, 123.21) mg/kg across China and had its largest value in autumn 81.33 (43.30, 121.28) mg/kg. Based on very limited observations, the SIN concentration showed a slight decrease (76.62 (59.20, 98.27) mg/kg) in winter compared with autumn. However, both CLM4.5 and CLM5.0 underestimated SIN concentrations throughout seasons (Figure 7). The seasonal changes of SIN concentration were roughly captured by CLM4.5 but not by CLM5.0 (Figure 7).

Both models showed no trends in the SIN across China from 1980 to 2010 (Figure 8). Even at global scale, most of the regions had minor changes in SIN from 1980 to 2005. However, CLM4.5 and CLM5.0 simulated different trends in SIN in some regions. For example, the SIN showed no trend in the tropical rainforests of Africa in the CLM4.5 model but showed decreasing trends in the CLM5.0 model (Figure 8).

We further analyzed the determinant processes of the SIN pool in the CLM4.5. The SIN pool showed a significant positive correlation with the net N balance between influxes and effluxes ( $p < 0.001$ , Figure 9b). N mineralization was the major replenishment to the SIN pool in CLM4.5, with a wide range from 0 to 65.38  $\text{gN}\cdot\text{m}^{-2}\cdot\text{year}^{-1}$  (Figure 9a). The simulated annual fixation ranged from 0 to 1.6  $\text{gN}\cdot\text{m}^{-2}\cdot\text{year}^{-1}$ . Atmospheric N deposition ranged from 0 to 2.11  $\text{gN}\cdot\text{m}^{-2}\cdot\text{year}^{-1}$ . The depletion of SIN mainly occurred by immobilization (from 0 to 42.45  $\text{gN}\cdot\text{m}^{-2}\cdot\text{year}^{-1}$ ) and plant uptake (from 0 to 26.15  $\text{gN}\cdot\text{m}^{-2}\cdot\text{year}^{-1}$ ). The contribution of SIN leaching (from 0 to 7.40  $\text{gN}\cdot\text{m}^{-2}\cdot\text{year}^{-1}$ ) and denitrification (from 0 to 1.14  $\text{gN}\cdot\text{m}^{-2}\cdot\text{year}^{-1}$ ) to SIN losses accounted for less than 0.05%.

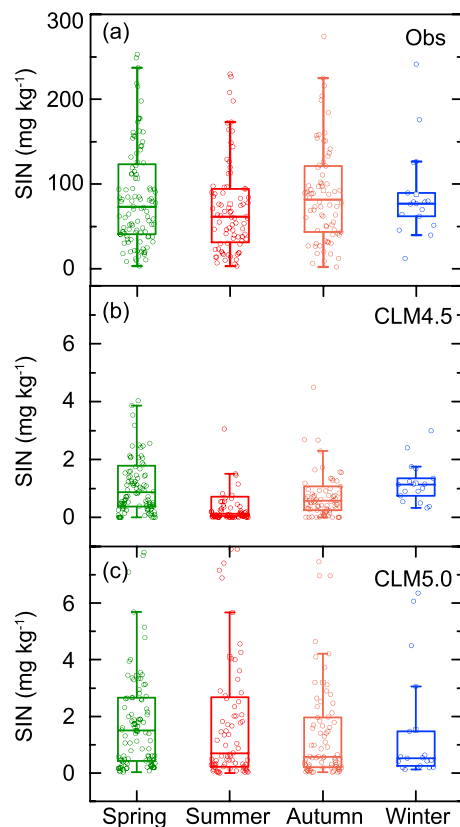


**Figure 7.** The seasonal variation of SIN from (a) observations, (b) CLM4.5, and (c) CLM5.0. Lower and upper edges of the boxes indicate the 25th and 75th percentiles, respectively. Bars outside the boxes represent the 10th and 90th percentiles. The dots in the box indicate the observed and simulated SIN status in corresponding grid cells. SIN = soil inorganic nitrogen; CLM = Community Land Model.

## 4. Discussion

### 4.1. Diagnosing Model Performance With the Spatial Distributions of SIN

This study shows a large spatial variation of the SIN on the regional scale (Figure 1). To our best knowledge, this is the first study to characterize the frequency distributions of the SIN in China (Figure 3b). The statistical properties of such skewed distributions, such as the median and quartiles, can be useful in diagnosing the model performance with SIN estimates. For example, there is approximately a fourfold difference between the upper and lower quartiles of SIN observations, and such a difference is comparable with that in CLM4.5 (approximately sixfolds) and CLM5.0 (approximately fivefolds; Figure 5a). However, the median of the observations is ~70-folds larger than that in the models. This result indicates that the models dramatically underestimated the size of the SIN pool, at least across China.

Interestingly, the SIN concentration is lowest in the regions with a MAT of approximately 10 °C (Figure 2a). In China, these regions are mainly covered by deserts (Hong et al., 2005; <http://www.chinamaps.org/>), which have a lower SIN than other biomes (Figure 1). This study found a positive correlation between the SIN concentration and MAP (Figure 2b), suggesting that water availability plays an important role in regulating the spatial variation of SIN. It is clear that the models not only underestimated the SIN concentration in all ecosystems but also could not capture well the differences among ecosystems (Figure 6).

### 4.2. Minor Long-Term Changes in SIN on a Regional Scale

The regional SIN across China shows no temporal trend during the past three decades (Figure 3). This result is surprising because China is one of the regions that has been experiencing the fastest environmental changes, especially the increasing atmospheric N deposition (Galloway et al., 2008; Liu et al., 2013; Lu et al., 2011). The results from meta-analysis show that SIN has insignificant or decreasing responses under chronic

treatments (Figure 4). Atmospheric N deposition could generally enhance SIN pool, but the increase in SIN is hard to maintain over the long run (Lu et al., 2011; Osullivan et al., 2011). Once the enrichment of SIN exceeds the retention ability, large losses of SIN through dissolved inorganic nitrogen leaching and gaseous emissions will be expected (Niu et al., 2016). Therefore, the responses of SIN under long-term N addition are diminishing (Figure 4d). This may explain the reason why SIN concentration shows minor changes over China in the past three decades although this region experienced long-term N deposition.

Similarly, long-term warming and elevated CO<sub>2</sub> concentration have insignificant effects on SIN (Figure 4). However, such a long-term neutral effect could be driven by different mechanisms. For example, elevated CO<sub>2</sub> concentration reduces soil N leaching and increases biological N fixation, but N<sub>2</sub>O emission is significantly increased (Liang et al., 2016). Warming directly enhances SIN through accelerating mineralization rate, but shifting in moisture condition under the chronic warming could trigger SIN losses (Bai et al., 2013; Shaver et al., 2000), leading to no responses of SIN in the long run (Bai et al., 2013). Experimental evidence from a 6-year soil warming at alpine tree line (Dawes et al., 2016) and a two-decade warming experiment in an Arctic system (Sistla et al., 2013) consistently suggest that warming induced increase in SIN can only be detected in the early stage.

Benchmarking the performance of C-N-coupled models is much more difficult than that of C-only models, mainly because SIN plays a decisive role in regulating many processes. In current C-N-coupled models, multiple SIN-based functions are applied to model different N processes in the simulation of the N cycle (Zaehle & Dalmonech, 2011; Niu et al., 2016). For instance, the equations governing N losses in some models have a proportional relationship with SIN concentration. Besides, SIN supply is critical in nutritional feedback

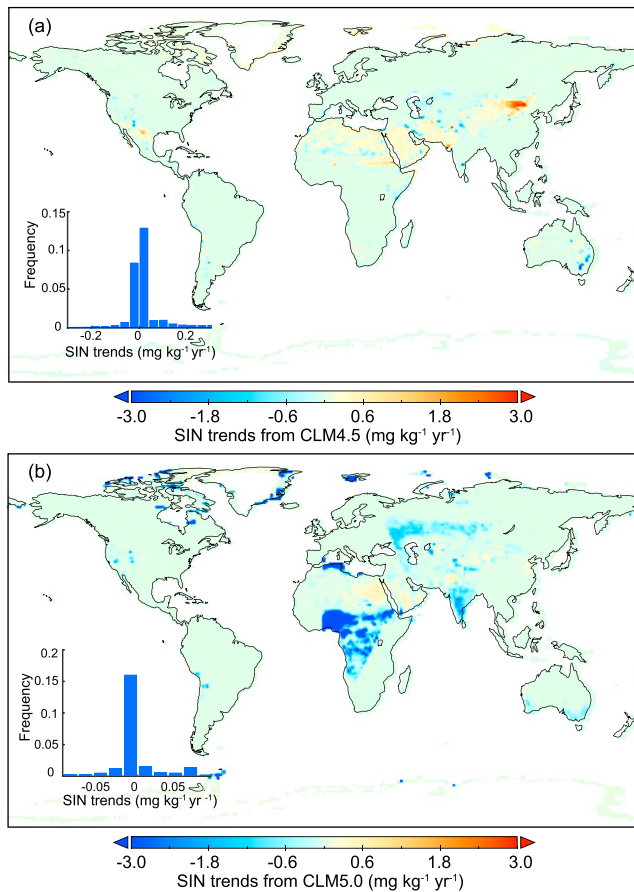


**Figure 8.** The spatial pattern of SIN trends simulated from CLM4.5 (a) and CLM5.0 (b) at a global scale. The inserted panels show the frequency distribution of SIN trends. SIN = soil inorganic nitrogen; CLM = Community Land Model.

constraining plant C uptake; thus, current C-N models commonly predict limited terrestrial C storage via N availability (Thornton et al., 2007; Zaehle et al., 2014). However, the simulations of SIN from short-term to long-term scale are poorly constrained by suitable observations. In our research, the minor long-term changes of SIN concentration on the regional scale (Figure 3) can be used as benchmarks for C-N-coupled models. The constructed data set is by no means conclusive, but it calls for a full evaluation of N cycles at multiple time and spatial scales. We recommend future experimental studies to simultaneously measure multiple N processes and to explore the mechanisms driving the dynamics of SIN over short term to long term, especially under different global-change factors.

#### 4.3. Improving the Estimate of SIN in Global Biogeochemical Models

The known underestimations of SIN in both CLM4.5 and CLM5.0 are helpful to improve their simulations on ecosystem N cycling across China. The pool size of SIN is collectively determined by the influxes, such as mineralization, fixation, and atmospheric deposition, and the effluxes, such as immobilization, plant uptake, denitrification, and leaching (Figure 7). Thus, the modelers can determine the major reasons for the underestimations by comparing these N processes against observations. In this study, we further estimated the annual mean soil N mineralization rate across China as  $\sim 121.73$  to  $300.27 \text{ gN}\cdot\text{m}^{-2}\cdot\text{year}^{-1}$  based on the synthesized mineralization data (Liu et al., 2016) and the national mean bulk density (Chai & He, 2016). This estimate is approximately fivefold larger than the simulated soil N mineralization rate by CLM4.5 (Figure 7). In addition, the rate of biological N fixation ranges from 0 to  $\sim 11 \text{ gN}\cdot\text{m}^{-2}\cdot\text{year}^{-1}$  in Eastern Asia (Cleveland et al., 1999, 2013), which is also obviously underestimated by CLM4.5 (Figure 7). Only the rates of atmospheric N deposition are comparable with nationwide observations ( $\sim 2.1 \text{ gN}\cdot\text{m}^{-2}\cdot\text{year}^{-1}$ ; Liu et al., 2013).

The underestimation of SIN in these models may also result from their overestimates of the depletion processes of SIN. As shown in Figure 7, the majority of SIN in the CLM4.5 is incorporated into organisms through immobilization and plant uptake, rather than what is lost through denitrification and leaching (Figure 7a). This result indicates the potential for SIN retention in the CLM4.5. However, we are limited in evaluating SIN effluxes due to the sparse observational database. A promising way is to apply  $^{15}\text{N}$  tracer field data for quantitatively evaluating the fate of SIN in C-N coupled modes (Cheng et al., 2018; Thomas et al., 2013; Zhu et al., 2017). For example, Cheng et al. (2018) has applied the long-term  $^{15}\text{N}$  tracer field experimental data as benchmarks to evaluate the simulated N cycling dynamics in CLM5.0. Their results have revealed that CLM5.0 overestimates the recovery of N in plants and underestimates the recovery in the soil, indicating the existing flaws in partitioning SIN among plant, soils, and N-loss processes. Earlier studies have consistently shown the biases in CLM-CN in simulating the fates of SIN (Thomas et al., 2013), especially the unrealistically high SIN losses. The significant underestimation of SIN in CLM from our study may partially explain the persistent N limitation in CLM which is detected by Thomas et al. (2013). These evidence together with our study collectively indicate that the SIN dynamics simulated from CLM need improvements.

The SIN pool size is the resultant of multiple N transformation processes. An accurate representation of multiple N-transformation processes is the cornerstone for realistically simulating SIN. In both CLM4.5 and CLM5.0, the most influential feature on SIN dynamics is the demand-based competition for the limiting resources (Oleson et al., 2013; Thornton et al., 2007). The potential SIN demand from plant uptake, immobilization, nitrification, and denitrification are assumed to be satisfied simultaneously. When SIN is insufficient to meet the total demand, the potential SIN available to a particular N process is downregulated based on the proportion of the individual demand to the total demand. A constant fraction of the remaining SIN is

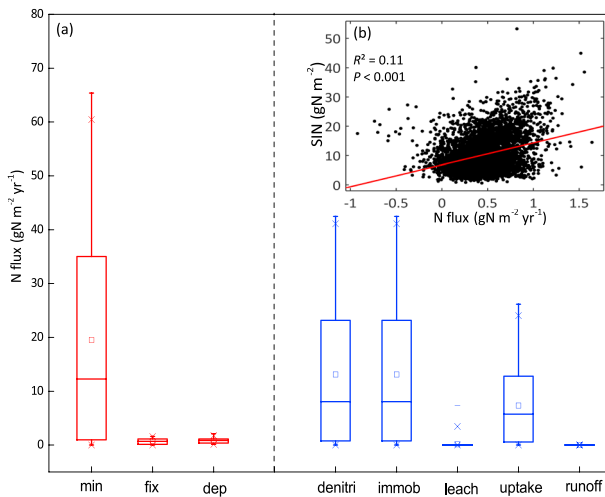


**Figure 9.** The annual mean nitrogen fluxes in China over 26 years simulated by CLM4.5 (a). The red boxplots represent the influxes of the SIN pool, that is, mineralization, fixation, and nitrogen deposition. The blue boxplots represent the effluxes, that is, immobilization, plant uptake, denitrification, and leaching. The value of influxes minus effluxes was then correlated with SIN condition (b). SIN = soil inorganic nitrogen.

dissolved in soil water and will be lost through leaching (Oleson et al., 2013; CLM5.0 technical description). The demand-based approach simplifies the complex nutrients competition among multiple N processes, resulting in the unrealistic simulation on the SIN fates (Cheng et al., 2018; Zhu et al., 2017). A more sophisticated representation of the nutrient competition among plant, soil, and microbe would be likely to improve the models' performance on simulating multiple N transformations (Zhu et al., 2016, 2017). A recent developed framework, the Equilibrium Chemistry Approximation theory, shows its superiority in capturing multiple N transformations when considering the affinity of different enzymes to SIN.

Although the representations of N fixation, plant N-acquisition strategy (FUN), and plant stoichiometry (FlexCN) have been improved in CLM5.0 (CLM5.0 technical description), it failed to match the observed SIN pool across China (Figure 5). Besides, these modifications of model's processes cause additional uncertainties in simulating the seasonal variations (Figure 7) and the spatial trends (Figure 8) of SIN. The simulated SIN from the CLMs is all the available nitrogen for multiple N and C processes therefore is pivotal in regulating the feedbacks of terrestrial ecosystem to climate changes. The unrealistic estimation on SIN might lead to biases in modeling the terrestrial C-N interactions. The discrepancy between models' simulation and field observations reflects the uncertain-

ties in models' structure, parameters, and initial conditions (Luo et al., 2012). These uncertainties are not unique to the CLMs but to many other C-N-coupled models (Zaehle & Dalmonech, 2011). To narrow the uncertainties in simulating the nitrogen availability, incorporating new theoretical framework into the models together with integrating field observations to constrain models is highly recommended (Sulman et al., 2017). Especially, if the N isotope discrimination is included in the C-N-coupled models, the new synthesized foliar N concentrations and isotope ratio ( $\delta^{15}\text{N}$ ) data set by Craine et al. (2018) could be valuable for evaluating the plant-related N processes.

## 5. Conclusions

In summary, this study reveals the long-term nonsignificant changes of the SIN on a regional scale. Such a property of the SIN is then used to evaluate two versions of CLM (i.e., CLM4.5 and CLM5.0). The results from our data-model comparison show that both CLM4.5 and CLM5.0 significantly underestimate SIN concentration in China. In addition, huge biases are existed in simulating the seasonal variation and spatial pattern of SIN. The underestimations of the SIN concentration by the two state-of-the-art global land models are largely due to the low rates of N mineralization and biological fixation. However, to explain these uncertainties in a mechanical way, further studies need to decompose the modeled SIN into its related processes.

The dynamic of SIN is the balance of multiple N-transformation processes. An accurate estimation on the SIN pool needs more realistic representations of multiple N-transformation processes. Studies on single N processes are too isolated to inform models because all N transformation processes are integrated with each other (Jansson & Petsson, 1982). Thus, this study recommends more future experimental and modeling studies to explore the role of SIN in regulating multiple N processes in terrestrial ecosystems.

## References

- Aber, J., McDowell, W., Nadelhoffer, K., Magill, A., Berntson, G., Kamakea, M., et al. (1998). Nitrogen saturation in temperate forest ecosystems. *Bioscience*, 48(11), 921–934. <https://doi.org/10.2307/1313296>
- Baddeley, A. (2007). *Spatial point processes and their applications*. In *lecture notes in mathematics: Stochastic geometry*, (Vol. 1892, pp. 1–75). Springer.
- Bai, E., Li, S., Xu, W., Li, W., Dai, W., & Jiang, P. (2013). A meta-analysis of experimental warming effects on terrestrial nitrogen pools and dynamics. *New Phytologist*, 199(2), 441–451. <https://doi.org/10.1111/nph.12252>
- Cain, M. L., Subler, S., Evans, J. P., & Fortin, M.-J. (1999). Sampling spatial and temporal variation in soil nitrogen availability. *Oecologia*, 118(4), 397–404. <https://doi.org/10.1007/s004420050741>

## Acknowledgments

This work was financially supported by the National Key R&D Program of China (2017YFA0604603), National Natural Science Foundation of China (31722009 and 41630528), the National 1000 Young Talents Program of China, and the Fok Ying-Tong Education Foundation for Young Teachers in the Higher Education Institutions of China (grant 161016). The SIN data obtained from the Chinese Ecosystem Research Network are available via <http://www.cern.ac.cn/0index/index.asp> or by contacting the corresponding author Jianyang Xia (jyxia@des.ecnu.edu.cn). Climate data of precipitation and temperature is downloaded online ([https://crudata.uea.ac.uk/cru/data/hrg/cru\\_ts\\_3.23/](https://crudata.uea.ac.uk/cru/data/hrg/cru_ts_3.23/)). Analysis for Figure is produced with the synthesized data from Bai et al. (2013), Lu et al. (2011), and Liang et al. (2016).

- Chai, H., & He, N. P. (2016). Evaluation of soil bulk density in China terrestrial ecosystems for determination of soil carbon storage on a regional scale. *Acta Ecologica Sinica*, *36*(13).
- Cheng, S. J., Hess, P. G., Wieder, W. R., Thomas, R. Q., Nadelhoffer, K. J., Vira, J., et al. (2018). Decadal impacts of nitrogen additions on temperate forest carbon sinks: A data-model comparison. *Biogeosciences Discussions*, 1–38. <https://doi.org/10.5194/bg-2018-505>
- Cleveland, C. C., Houlton, B. Z., Smith, W. K., Marklein, A. R., Reed, S. C., Parton, W., et al. (2013). Patterns of new versus recycled primary production in the terrestrial biosphere. *Proceedings of the National Academy of Sciences*, *110*(31), 12733–12737. <https://doi.org/10.1073/pnas.1302768110>
- Cleveland, C. C., Townsend, A. R., Schimel, D. S., Fisher, H., Howarth, R. W., Hedin, L. O., et al. (1999). Global patterns of terrestrial biological nitrogen (N<sub>2</sub>) fixation in natural ecosystems. *Global Biogeochemical Cycles*, *13*(2), 623–645. <https://doi.org/10.1029/1999GB900014>
- Craine, J. M., Elmore, A. J., Wang, L., Aranibar, J., Bauters, M., Boeckx, P., et al. (2018). Isotopic evidence for oligotrophication of terrestrial ecosystems. *Nature Ecology and Evolution*, *2*(11), 1735–1744. <https://doi.org/10.1038/s41559-018-0694-0>
- Dawes, M. A., Schleppli, P., Hattenschwiler, S., Rixen, C., & Hagedorn, F. (2016). Soil warming opens the nitrogen cycle at the alpine treeline. *Global Change Biology*, *23*, 421–434. <https://doi.org/10.1111/gcb.13365>
- Delgadobaquerizo, M., & Gallardo, A. L. (2011). Depolymerization and mineralization rates at 12 Mediterranean sites with varying soil N availability. A test for the Schimel and Bennett model. *Soil Biology & Biochemistry*, *43*(3), 693–696. <https://doi.org/10.1016/j.soilbio.2010.11.030>
- Dise, N. B., & Wright, R. F. (1995). Nitrogen leaching from European forests in relation to nitrogen deposition. *Forest Ecology and Management*, *71*(1-2), 153–161. [https://doi.org/10.1016/0378-1127\(94\)06092-W](https://doi.org/10.1016/0378-1127(94)06092-W)
- Dommergues, Y. R., & Ganry, F. (1986). Biological nitrogen fixation and soil fertility maintenance. In A. U. Mokwunye, & P. L. G. Vlek (Eds.), *Management of nitrogen and phosphorus fertilizers in Sub-Saharan Africa: Proceedings of a symposium, held in Lome, Togo, March 25–28, 1985* (pp. 95–115). Dordrecht: Springer Netherlands. [https://doi.org/10.1007/978-94-009-4398-8\\_5](https://doi.org/10.1007/978-94-009-4398-8_5)
- Du, Z., Weng, E., Jiang, L., Luo, Y., Xia, J., & Zhou, X. (2018). Carbon–nitrogen coupling under three schemes of model representation: A traceability analysis. *Geoscientific Model Development*, *11*(11), 4399–4416. <https://doi.org/10.5194/gmd-11-4399-2018>
- Friedlingstein, P., Cox, P., Betts, R., Bopp, L., von Bloh, W., Brovkin, V., et al. (2006). Climate-carbon cycle feedback analysis: Results from the C4MIP model Intercomparison. *Journal of Climate*, *19*(14), 3337–3353. <https://doi.org/10.1175/jcli3800.1>
- Friedlingstein, P., Meinshausen, M., Arora, V. K., Jones, C. D., Anav, A., Liddicoat, S. K., & Knutti, R. (2014). Uncertainties in CMIP5 climate projections due to carbon cycle feedbacks. *Journal of Climate*, *27*(2), 511–526. <https://doi.org/10.1175/jcli-d-12-00579.1>
- Galloway, J. N., Townsend, A. R., Erisman, J. W., Bekunda, M., Cai, Z., Freney, J. R., et al. (2008). Transformation of the nitrogen cycle: Recent trends, questions, and potential solutions. *Science*, *320*(5878), 889–892. <https://doi.org/10.1126/science.1136674>
- Greaver, T. L., Clark, C. M., Compton, J. E., Vallano, D., Talhelm, A. F., Weaver, C. P., et al. (2016). Key ecological responses to nitrogen are altered by climate change. *Nature Climate Change*, *6*(9), 836–843. <https://doi.org/10.1038/nclimate3088>
- Gruber, N., & Galloway, J. N. (2008). An Earth-system perspective of the global nitrogen cycle. *Nature*, *451*(7176), 293–296. <https://doi.org/10.1038/nature06592>
- Hajari, E., Snyman, S. J., & Watt, M. P. (2014). Inorganic nitrogen uptake kinetics of sugarcane (*Saccharum* spp.) varieties under in vitro conditions with varying N supply. *Plant Cell, Tissue and Organ Culture (PCTOC)*, *117*(3), 361–371. <https://doi.org/10.1007/s11240-014-0445-0>
- Hedges, L. V., Gurevitch, J., & Curtis, P. S. (1999). The meta-analysis of response ratios in experimental ecology. *Ecology*, *80*(4), 1150–1156. [https://doi.org/10.1890/0012-9658\(1999\)080\[1150:TMAORR\]2.0.CO;2](https://doi.org/10.1890/0012-9658(1999)080[1150:TMAORR]2.0.CO;2)
- Hong, Y., Nix, H. A., Hutchinson, M. F., & Booth, T. H. (2005). Spatial interpolation of monthly mean climate data for China. *International Journal of Climatology*, *25*(10), 1369–1379. <https://doi.org/10.1002/joc.1187>
- Houlton, B. Z., Morford, S. L., & Dahlgren, R. A. (2018). Convergent evidence for widespread rock nitrogen sources in Earth's surface environment. *Science*, *360*(6384), 58–62. <https://doi.org/10.1126/science.aan4399>
- Hungate, B. A., Dukes, J. S., Shaw, M. R., Luo, Y., & Field, C. B. (2003). Nitrogen and climate change. *Science*, *302*(5650), 1512–1513. <https://doi.org/10.1126/science.1091390>
- Hurrell, J. W., Holland, M. M., Gent, P. R., Ghan, S., Kay, J. E., Kushner, P. J., et al. (2013). The community Earth system model: A framework for collaborative research. *Bulletin of the American Meteorological Society*, *94*(9), 1339–1360. <https://doi.org/10.1175/BAMS-D-12-00121.1>
- Jansson, S. L., & Petsson, J. (1982). Mineralization and immobilization of soil nitrogen. *Agronomy*, *22*, 229–252.
- Jorgensen, B. H.-S. E. (1993). 2. Biological nitrification and denitrification. In B. Halling-Sorensen, & S. E. Jorgensen (Eds.), *Studies in environmental science*, (Vol. 54, pp. 43–53). Elsevier.
- Keeney, D. R. (1982). Nitrogen-availability indices. In A. Klute (Ed.), *Methods of soil analysis, part, chemical & microbiological properties*, (pp. 711–733). Madison, WI: ASA and SSSA.
- Koven, C. D., Riley, W. J., Subin, Z. M., Tang, J. Y., Torn, M. S., Collins, W. D., et al. (2013). The effect of vertically resolved soil biogeochemistry and alternate soil C and N models on C dynamics of CLM4. *Biogeosciences*, *10*(11), 7109–7131. <https://doi.org/10.5194/bg-10-7109-2013>
- Liang, J., Qi, X., Souza, L., & Luo, Y. (2016). Processes regulating progressive nitrogen limitation under elevated carbon dioxide: A meta-analysis. *Biogeosciences*, *13*(9), 2689–2699. <https://doi.org/10.5194/bg-13-2689-2016>
- Liu, X., Zhang, Y., Han, W., Tang, A., Shen, J., Cui, Z., et al. (2013). Enhanced nitrogen deposition over China. *Nature*, *494*(7438), 459–462. <https://doi.org/10.1038/nature11917>
- Liu, Y., Wang, C., He, N., Wen, X., Gao, Y., Li, S., et al. (2016). A global synthesis of the rate and temperature sensitivity of soil nitrogen mineralization: Latitudinal patterns and mechanisms. *Global Change Biology*, *23*, 455–464. <https://doi.org/10.1111/gcb.13372>
- Lu, M., Yang, Y., Luo, Y., Fang, C., Zhou, X., Chen, J., et al. (2011). Responses of ecosystem nitrogen cycle to nitrogen addition: A meta-analysis. *New Phytologist*, *189*(4), 1040–1050. <https://doi.org/10.1111/j.1469-8137.2010.03563.x>
- Luo, Y., Ahlstrom, A., Allison, S. D., et al. (2016). Toward more realistic projections of soil carbon dynamics by Earth system models. *Global Biogeochemical Cycles*, *30*, 40–56. <https://doi.org/10.1002/2015GB005239>
- Luo, Y., Su, B., Currie, W. S., et al. (2004). Progressive nitrogen limitation of ecosystem responses to rising atmospheric carbon dioxide. *Bioscience*, *54*(8), 731. [https://doi.org/10.1641/0006-3568\(2004\)054\[0731:PNLOER\]2.0.CO;2](https://doi.org/10.1641/0006-3568(2004)054[0731:PNLOER]2.0.CO;2)
- Luo, Y. Q., Randerson, J. T., Abramowitz, G., Bacour, C., Blyth, E., Carvalhais, N., et al. (2012). A framework for benchmarking land models. *Biogeosciences*, *9*(10), 3857–3874. <https://doi.org/10.5194/bg-9-3857-2012>
- Morales, J., Benavides-picione, R., Dar, M., et al. (2014). Random positions of dendritic spines in human cerebral cortex. *The Journal of Neuroscience*, *34*(30), 10078–10084. <https://doi.org/10.1523/JNEUROSCI.1085-14.2014>

- Niu, S., Classen, A. T., Dukes, J. S., Kardol, P., Liu, L., Luo, Y., et al. (2016). Global patterns and substrate-based mechanisms of the terrestrial nitrogen cycle. *Ecology Letters*, *19*(6), 697–709. <https://doi.org/10.1111/ele.12591>
- Oleson, K. W., Lawrence, D. M., & Bonan, G. B. (2013). Technical description of version 4.5 of the Community Land Model (CLM). NCAR tech. Note NCAR/TN-503+STR. National Center for Atmospheric Research, Boulder. *Geophysical Research Letters*, *37*, 256–265.
- Osullivan, O. S., Horswill, P., Phoenix, G. K., Lee, J. A., & Leake, J. R. (2011). Recovery of soil nitrogen pools in species-rich grasslands after 12 years of simulated pollutant nitrogen deposition: A 6-year experimental analysis. *Global Change Biology*, *17*(8), 2615–2628. <https://doi.org/10.1111/j.1365-2486.2011.02403.x>
- Peñuelas, J., Poulter, B., Sardans, J., Ciais, P., van der Velde, M., Bopp, L., et al. (2013). Human-induced nitrogen–phosphorus imbalances alter natural and managed ecosystems across the globe. *Nature Communications*, *4*(1), 2934. <https://doi.org/10.1038/ncomms3934>
- Schlesinger, W. H., & Bernhardt, E. S. (2013). Chapter 6—The biosphere: Biogeochemical cycling on land. In *Biogeochemistry* (Third ed. pp. 173–231). Boston: Academic Press. <https://doi.org/10.1016/B978-0-12-385874-0.00006-6>
- Shaver, G. R., Canadell, J., Chapin, F. S., et al. (2000). Global warming and terrestrial ecosystems: A conceptual framework for analysis. *Bioscience*, *50*(10), 871–882. [https://doi.org/10.1641/0006-3568\(2000\)050\[0871:GWATEA\]2.0.CO;2](https://doi.org/10.1641/0006-3568(2000)050[0871:GWATEA]2.0.CO;2)
- Sistla, S. A., Moore, J. C., Simpson, R. T., Gough, L., Shaver, G. R., & Schimel, J. P. (2013). Long-term warming restructures Arctic tundra without changing net soil carbon storage. *Nature*, *497*(7451), 615–618. <https://doi.org/10.1038/nature12129>
- Sulman, B. N., Brzostek, E. R., Medici, C., Shevliakova, E., Menge, D. N., & Phillips, R. P. (2017). Feedbacks between plant N demand and rhizosphere priming depend on type of mycorrhizal association. *Ecology Letters*, *20*(8), 1043–1053. <https://doi.org/10.1111/ele.12802>
- Technical description of version 5.0 of the Community Land Model (CLM). (2018): 35 [http://www.cesm.ucar.edu/models/cesm2/land/CLM50\\_Tech\\_Note.pdf](http://www.cesm.ucar.edu/models/cesm2/land/CLM50_Tech_Note.pdf).
- Thomas, R. Q., Zaehle, S., Templer, P. H., & Goodale, C. L. (2013). Global patterns of nitrogen limitation: Confronting two global biogeochemical models with observations. *Global Change Biology*, *19*(10), 2986–2998. <https://doi.org/10.1111/gcb.12281>
- Thornton, P. E., Doney, S. C., Lindsay, K., Moore, J. K., Mahowald, N., Randerson, J. T., et al. (2009). Carbon-nitrogen interactions regulate climate-carbon cycle feedbacks: Results from an atmosphere-ocean general circulation model. *Biogeosciences*, *6*(10), 2099–2120. <https://doi.org/10.5194/bg-6-2099-2009>
- Thornton, P. E., Lamarque, J.-F., Rosenbloom, N. A., & Mahowald, N. M. (2007). Influence of carbon-nitrogen cycle coupling on land model response to CO<sub>2</sub> fertilization and climate variability. *Global Biogeochemical Cycles*, *21*, GB4018. <https://doi.org/10.1029/2006GB002868>
- Wang, Y. P., & Houlton, B. Z. (2009). Nitrogen constraints on terrestrial carbon uptake: Implications for the global carbon-climate feedback. *Geophysical Research Letters*, *36*, L24403. <https://doi.org/10.1029/2009GL041009>
- Wang, Y. P., & Pak, B. (2010). A global model of carbon, nitrogen and phosphorus cycles for the terrestrial biosphere. *Biogeosciences*, *7*(7), 2261–2282. <https://doi.org/10.5194/bg-7-2261-2010>
- Wieder, W. R., Cleveland, C. C., Smith, W. K., & Todd-Brown, K. (2015). Future productivity and carbon storage limited by terrestrial nutrient availability. *Nature Geoscience*, *8*(6), 441–444. <https://doi.org/10.1038/ngeo2413>
- Xia, J., & Wan, S. (2008). Global response patterns of terrestrial plant species to nitrogen addition. *New Phytologist*, *179*(2), 428–439. <https://doi.org/10.1111/j.1469-8137.2008.02488.x>
- Zaehle, S., & Dalmonech, D. (2011). Carbon–nitrogen interactions on land at global scales: Current understanding in modelling climate biosphere feedbacks. *Current Opinion in Environmental Sustainability*, *3*(5), 311–320. <https://doi.org/10.1016/j.cosust.2011.08.008>
- Zaehle, S., & Friend, A. D. (2010). Carbon and nitrogen cycle dynamics in the O-CN land surface model: 1. Model description, site-scale evaluation, and sensitivity to parameter estimates. *Global Biogeochemical Cycles*, *24*, GB1005. <https://doi.org/10.1029/2009GB003521>
- Zaehle, S., Medlyn, B. E., De Kauwe, M. G., et al. (2014). Evaluation of 11 terrestrial carbon-nitrogen cycle models against observations from two temperate free-air CO<sub>2</sub> enrichment studies. *New Phytologist*, *202*(3), 803–822. <https://doi.org/10.1111/nph.12697>
- Zhu, Q., Riley, W. J., & Tang, J. (2017). A new theory of plant–microbe nutrient competition resolves inconsistencies between observations and model predictions. *Ecological Applications*, *27*(3), 875–886. <https://doi.org/10.1002/eap.149>
- Zhu, Q., Riley, W. J., Tang, J., & Koven, C. D. (2016). Multiple soil nutrient competition between plants, microbes, and mineral surfaces: Model development, parameterization, and example applications in several tropical forests. *Biogeosciences*, *13*(1), 341–363. <https://doi.org/10.5194/bg-13-341-2016>